Available online at www.sciencedirect.com
SCIENCE DIRECT
Mathematical and Computer Modelling 40 (2004) 941–951
MATHEMATICAL AND COMPUTER MODELLING
www.elsevier.com/locate/mcm

A Semi-Implicit Space-Time CE-SE Method to Improve Mass Conservation through Tapered Ducts in Internal Combustion Engines

S. JEREZ, J. V. ROMERO AND M. D. ROSELLÓ
Instituto de Matemática Multidisciplinar
Universidad Politécnica de Valencia, Spain
<siljega><jvromero><drosello>@mat.upv.es

F. J. ARNAU
CMT - Máquinas y Motores Térmicos
Universidad Politécnica de Valencia, Spain
farnau@mot.upv.es

(Received March 2004; accepted April 2004)

Abstract—In this work, we present a semi-implicit method based on the CE-SE numerical scheme (space time conservation-element and solution-element). In particular, we apply this method to a hyperbolic system that models the dynamics of an unsteady flow along a tapered duct with friction and heat transfer. Conditions on the scheme in order to get real numerical solutions are given. The improvement that offers the semi-implicit method versus the scheme CE-SE is compared by means of numerical simulations based on the property of the mass conservation.

Keywords—CE-SE scheme, Semi-implicit method, Hyperbolic system, Tapered ducts

1. INTRODUCTION

The numerical simulation of wave dynamics through the engine ducts represents an essential tool to assist the design and optimization of new internal combustion engines. The use of wave action models throughout the automotive industry has notably increased in the last years, due to the important progress made in terms of reliability, accuracy, robustness, and flexibility.

These models solve the one-dimensional unsteady nonhomeotropic mass, momentum, and energy conservation laws, which are the equations that govern the flow dynamic and form a nonhomogeneous hyperbolic system. The hypothesis of one-dimensional flow allows a great simplification of the problem and an important reduction in computational time. In comparison with

This work has been partially supported by the Spanish M.C.Y.T. Grants DPI2001–2703–C02–02 and DPI2003–07153–C02–02.

0895-7177/04/$ - see front matter Typeset by AMS-TEX
doi:10.1016/j.mcm.2004.04.001

CFD codes (three-dimensional calculations), wave action models are able to solve the thermo-fluiddynamic of whole engines with reasonable computational requirements and predict the interaction between the different elements. This characteristic allows a quick analysis of the engine behaviour with good accuracy.

Different numerical frameworks can be used to carry out these calculations. The most utilized, especially in engine modelizations, are the finite-difference schemes due to their good relationship between accuracy and speed. Despite this, it is interesting to point out an innovative numerical method for solving conservation law such as the method of space-time conservation element and solution element (abbreviated as the CE-SE method) [1,2] which is different in both concept and methodology from well-established traditional high resolution methods such as flux corrected techniques (FCT), total variation diminishing schemes (TVD), etc. [3,4]. Neither a flux limiter nor a characteristic based technique are involved. In the CE-SE method, the main emphasis is on solving the integral form of the conservation law in the space-time domain, although the differential form is also considered. As a direct statement of the integral form, the space-time flux is conserved globally in the space-time domain. On the other hand, the traditional methods that address flux conservation focus only on the conservation of spatial flux. For the CE-SE method, highly accurate numerical solutions have been obtained for various flow problems involving discontinuities, such as shock waves, contact surfaces, and even their interactions in comparison with traditional schemes. On the other hand, this method presents important conservation problems when the section of the duct varies, overall, when the derivate of the section does not exist [5].

In tapered ducts, when the conical angle is too large, the one-dimensional flow assumption can be inappropriate due to the axial symmetry flow effects. Nevertheless, even with low conical angles, it is well known that tapered duct calculation causes mass conservation problems, which can be increased with the consideration of pulsating flow, typical in automotive engines. These types of ducts are often used in engines in order to benefit from the pressure pulse reflection, especially in the exhaust system of two-stroke engines. For this reason, fast and accurate numerical methods are required.

In this paper, a semi-implicit 1-D CE-SE solver for nonhomogeneous conservation laws is developed and compared with the original version of the CE-SE method in terms of mass conservation. The aim of this semi-implicit version of the proposed scheme is to minimize these conservation problems. In order to achieve this objective, fewer approximations will be used to develop the method besides a simple smooth technique being adopted where the derivative of the section does not exist. Before the comparison, we will show that there is real numerical solution with the requirement of the CFL condition. Finally, the flow on different conical ducts have been calculated with both schemes and the error on mass conservation has been compared at several points of the ducts. The scheme proposed is focused on solving flow dynamic throughout engine ducts. For this reason, the conical angle chosen for the modelled ducts was similar to the conical angle of typical engine ducts. On the other hand, the main characteristic of the flow throughout the engine ducts is its pulsating behavior [6]. To take this behavior into account, the calculation has been carried out with impulsive flow.

2. MATHEMATICAL MODEL

The problem that describes the behavior of unsteady one-dimensional flow of a perfect gas in a tapered duct with friction and heat transfer is modelled by means of the following nonlinear hyperbolic system of differential equations [4]

$$\begin{aligned} W_t(x,t) + F_x(W(x,t)) + S(W(x,t)) = 0, \qquad & x \in [b_1, b_2] \subset \mathbb{R}, \quad 0 < t \leq T < +\infty, \\ W(x,0) &= W_0(x), \\ W(b_1,t) &= H(t), \\ W(b_2,t) &= G(t), \end{aligned} \tag{1}$$

with $S(W) = C_1(W) + C_2(W)$,

$$W = \begin{pmatrix} \rho \\ \rho u \\ \rho\frac{u^2}{2} + \frac{p}{\gamma - 1} \end{pmatrix}, \qquad F(W) = \begin{pmatrix} \rho u \\ \rho u^2 + p \\ u\left(\rho\frac{u^2}{2} + \frac{\gamma p}{\gamma - 1}\right) \end{pmatrix},$$
$$C_1(W) = \begin{pmatrix} \rho u \delta \\ \rho u^2 \delta \\ u\left(\rho\frac{u^2}{2} + \frac{\gamma p}{\gamma - 1}\right)\delta \end{pmatrix}, \quad \text{and} \quad C_2(W) = \begin{pmatrix} 0 \\ g\rho \\ -q\rho \end{pmatrix}, \tag{2}$$

where x: spatial dimension, t: time dimension, $\rho = \rho(x,t)$: density of the fluid, $p = p(x,t)$: pressure of the fluid, $u = u(x,t)$: velocity of the fluid, $A = A(x)$: area of the cross section of the duct, γ: ratio of specific heats, $g = 2f_r|u|u/D$: term with dimensions of acceleration taking into account the friction of the wall, $D = D(x)$: diameter of the duct, f_r: friction coefficient, $q = q(x,t)$: heat transfer term through the walls defined by heat transfer coefficient, h, and the temperature of the wall $T_p = T_p(x)$. The variation of the area of the section is given by the term δ, defined by

$$\delta = \frac{1}{A}\frac{dA}{dx}.$$

In system (1),(2), W is the vector of variables (density, momentum, and total energy), $F(W)$ is the flux vector, $C_1(W)$ represents the terms concerning to the variation of section of the duct and $C_2(W)$ involves the friction and heat transfer terms.

Finally, we write the initial and boundary conditions also in vectorial form for the resolution of the problem,

- Initial Condition:

$$W(x,0) = \begin{pmatrix} \rho(x,0) \\ p(x,0) \\ u(x,0) \end{pmatrix}, \qquad \forall x \in [b_1, b_2]\,. \tag{3}$$

- Boundary Conditions:

$$H(t) = \begin{pmatrix} \rho(b_1,t) \\ p(b_1,t) \\ u(b_1,t) \end{pmatrix}, \quad G(t) = \begin{pmatrix} \rho(b_2,t) \\ p(b_2,t) \\ u(b_2,t) \end{pmatrix}, \qquad \forall 0 < t \leq T. \tag{4}$$

3. SEMI-IMPLICIT CE-SE METHOD

In this section, we develop the semi-implicit numerical scheme based on the CE-SE method [1] applying it to system (1),(2). Let us rewrite the flux vector and the source term as functions of $W = [\omega_1, \omega_2, \omega_3]^\top$ in the following way:

$$F = F(W) = \begin{pmatrix} \omega_2 \\ (\gamma - 1)\omega_3 + \frac{(3-\gamma)}{2}\frac{\omega_2^2}{\omega_1} \\ \gamma\frac{\omega_3\omega_2}{\omega_1} - \frac{(\gamma-1)}{2}\frac{\omega_2^3}{\omega_1^2} \end{pmatrix}, \tag{5}$$

$$S = S(W) = \begin{pmatrix} \omega_2\delta \\ \left(\frac{\omega_2^2}{\omega_1}\right)\delta + \frac{2f_r}{D}\frac{\omega_2|\omega_2|}{\omega_1} \\ \left(\gamma\frac{\omega_3\omega_2}{\omega_1} - \frac{(\gamma-1)}{2}\frac{\omega_2^3}{\omega_1^2}\right)\delta + \frac{4h}{D}\left[\frac{(\gamma-1)}{R}\left(\frac{\omega_3}{\omega_1} - \frac{1}{2}\left(\frac{\omega_2}{\omega_1}\right)^2\right) - T_p\right] \end{pmatrix}. \tag{6}$$

We take a fixed spatial variation, Δx, and calculate the temporal variation, $(\Delta t)_n$, verifying in each step of time, n, the CFL condition

$$\frac{(\Delta t)_n}{\Delta x}\left[\max_{x\in[b_1,b_2]}(|u|+|a|)\right]=\tau, \tag{7}$$

where a is the sound speed and τ is a positive real number such that $0<\tau\leq 1$. The domain $[b_1,b_2]\times[0,T]$ is discretized by a mesh formed by a set of points or nodes, (x_j,t^n), where

$$x_j=b_1+j(\Delta x),\qquad j=0,\frac{1}{2},1,\ldots,M,\ \text{with } M=\frac{b_2-b_1}{\Delta x}, \tag{8a}$$

$$t^0=0,\quad t^n=t^{n-1/2}+\frac{(\Delta t)_n}{2},\qquad n=\frac{1}{2},1,\frac{3}{2},\ldots,N, \tag{8b}$$

where N satisfies that

$$T=t^{N-1/2}+\frac{(\Delta t)_N}{2}$$

with n and j alternatively an integer number and a semi-integer one, or vice versa (see Figure 1).

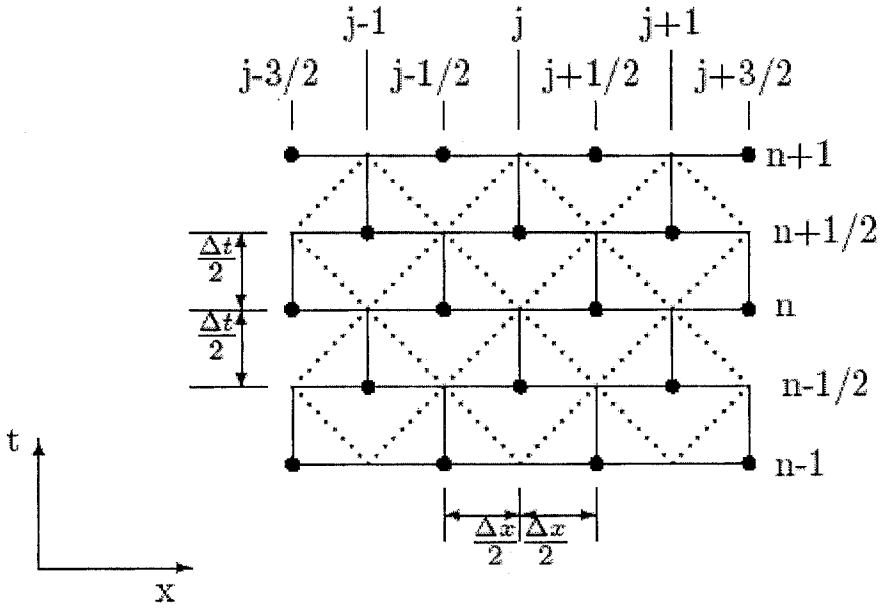

Figure 1. Discretization of the space-time domain.

The CE-SE method [2] discretizes the space-time domain into solution elements (SE), nonoverlapping opened rhombus centered in (x_j,t^n) where the numerical approximation is a simple linear function of space and time, and conservation elements (CE), nonoverlapping rectangles where the integral form of the system (1) is required, in each rectangle take part three different SEs (see Figures 1 and 2).

In each solution element, SE(j,n), each component of the vector $W(x,t)$ is approximated by means of first-order Taylor expansion:

$$\tilde{\omega}_k(x,t;j,n)=(\sigma_k)_j^n+(\alpha_k)_j^n(x-x_j)+(\beta_k)_j^n(t-t^n),\qquad k=1,2,3, \tag{9}$$

where

$$\begin{aligned}(\sigma_k)_j^n&=\tilde{\omega}_k\left(x_j,t^n;j,n\right),\\ (\alpha_k)_j^n&=\frac{\partial\tilde{\omega}_k}{\partial x}(x,t;j,n),\\ (\beta_k)_j^n&=\frac{\partial\tilde{\omega}_k}{\partial t}(x,t;j,n)=-\frac{\partial\tilde{f}_k}{\partial x}(x,t;j,n)-\tilde{s}_k(x,t;j,n).\end{aligned} \tag{10}$$

We denote the approximation vectors of F and S, in each $\mathrm{SE}(j,n)$, by $\tilde{F}$ and $\tilde{S}$, respectively, and we calculate them as follows [1].

$\tilde{F} = \left[\tilde{f}_1, \tilde{f}_2, \tilde{f}_3\right]$, such that $\tilde{F}(x,t;j,n) \approx F(\tilde{W}(x,t;j,n))$, obtained by means of Taylor expansion of two variables and truncating the terms of order superior.

$\tilde{S} = [\tilde{s}_1, \tilde{s}_2, \tilde{s}_3]$, such that $\tilde{S}(x,t;j,n) = S\left(\tilde{W}\left(x_j, t^n; j, n\right)\right)$, therefore $\tilde{S}$ is only defined by $(\sigma_k)_j^n$.

To obtain the numerical solution described in (9) it is necessary to know the coefficients $(\sigma_k)_j^n$, $(\alpha_k)_j^n$, and $(\beta_k)_j^n$, $\forall j,n$. Coefficients of the time step n are known and we are going to compute the coefficients of the next step, $n+1/2$.

For the calculation of $(\sigma_k)_j^{n+1/2}$, $k=1,2,3$, we utilize the resolution of the integral form of the system of differential equations, (1), in each $\mathrm{CE}(j,n+1/2)$ (see Figure 2),

$$\underbrace{\iint\limits_{\mathrm{CE}(j,n+1/2)} \frac{\partial \tilde{\omega}_k}{\partial t} + \frac{\partial \tilde{f}_k}{\partial x}\, dx\, dt}_{\text{(11a)}} + \underbrace{\iint\limits_{\mathrm{CE}(j,n+1/2)} \tilde{s}_k\, dx\, dt}_{\text{(11b)}} = 0, \qquad k=1,2,3. \tag{11}$$

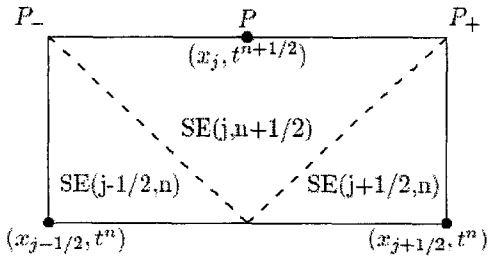

Figure 2. $\mathrm{CE}(j,n+1/2)$.

Applying *Green's theorem* [7] to (11a), we obtain the following path integral defined in the boundary of $\mathrm{CE}(j,n+1/2)$ for $k=1,2,3$ (see Figure 2),

$$\oint\limits_{\overline{\mathrm{CE}}(j,n+1/2)} -\tilde{\omega}_k\, dx + \tilde{f}_k\, dt = (\sigma_k)_j^{n+1/2}(\Delta x) - \left[(\sigma_k)_{j+1/2}^n + (\sigma_k)_{j-1/2}^n\right]\frac{(\Delta x)}{2} \tag{12}$$

$$+\left[(\alpha_k)_{j+1/2}^n - (\alpha_k)_{j-1/2}^n\right]\frac{(\Delta x)^2}{8} + \left[g_k\left(x_{j+1/2}, t; j+1/2, n\right) - g_k\left(x_{j-1/2}, t; j-1/2, n\right)\right],$$

where

$$g_1\left(x_{j+1/2}, t; j+1/2, n\right) = \sigma_2\frac{(\Delta t)}{2} + \beta_2\frac{(\Delta t)^2}{8}, \tag{13a}$$

$$g_2\left(x_{j+1/2}, t; j+1/2, n\right) = \left[(\gamma-1)\sigma_3 + \frac{(3-\gamma)}{2}\frac{\sigma_2^2}{\sigma_1}\right]\frac{(\Delta t)}{2} + \left[(\gamma-1)\beta_3 + \frac{(3-\gamma)}{2}\frac{\sigma_2}{\sigma_1}\left(2\beta_2 - \frac{\sigma_2\beta_1}{\sigma_1}\right)\right]\frac{(\Delta t)^2}{8}, \tag{13b}$$

$$g_3\left(x_{j+1/2}, t; j+1/2, n\right) = \left[\gamma\frac{\sigma_2\sigma_3}{\sigma_1} - \frac{(\gamma-1)}{2}\frac{\sigma_2^3}{\sigma_1^2}\right]\frac{\Delta t}{2} + \left[\gamma\frac{\sigma_3}{\sigma_1}\left(\frac{\beta_3\sigma_2}{\sigma_3} + \beta_2 - \frac{\beta_1\sigma_2}{\sigma_1}\right) + \frac{(\gamma-1)}{2}\frac{\sigma_2^2}{\sigma_1^2}\left(2\frac{\beta_1\sigma_2}{\sigma_1} - 3\beta_2\right)\right]\frac{(\Delta t)^2}{8}, \tag{13c}$$

where $\sigma_k = (\sigma_k)^n_{j+1/2}$ and $\beta_k = (\beta_k)^n_{j+1/2}$ for $k = 1, 2, 3$. To obtain $g_k(x_{j-1/2}, t; j-1/2, n)$, σ_k is replaced in (13) by $(\sigma_k)^n_{j-1/2}$ and β_k by $(\beta_k)^n_{j-1/2}$.

We decompose the integral (11b) as the sum of three integrals defined in each SE (see Figure 2) and approximate to each one of these integrals using the *mean value theorem* for integrals, using the value of the integrand in the center of the rhombus,

$$\iint\limits_{\mathrm{CE}(j,n+1/2)} \tilde{s}_k \, dx \, dt \cong \frac{(\Delta x)(\Delta t)}{4} \left[\frac{\tilde{s}_k(j+1/2, n) + \tilde{s}_k(j-1/2, n)}{2} + \tilde{s}_k(j, n+1/2) \right], \tag{14}$$

where

$$\tilde{s}_1(j, n+1/2) = \sigma_2 \delta_j, \tag{15a}$$

$$\tilde{s}_2(j, n+1/2) = \frac{\sigma_2^2}{\sigma_1}\delta_j + \frac{2 f_r}{D_j}\frac{\sigma_2|\sigma_2|}{\sigma_1}, \tag{15b}$$

$$\tilde{s}_3(j, n+1/2) = \left[\gamma \frac{\sigma_3 \sigma_2}{\sigma_1} - \frac{(\gamma-1)}{2}\frac{\sigma_2^3}{\sigma_1^2}\right]\delta_j + \frac{4h}{D_j}\left[\frac{(\gamma-1)}{R}\left(\frac{\sigma_3}{\sigma_1} - \frac{1}{2}\frac{\sigma_2^2}{\sigma_1^2}\right) - (T_p)_j\right], \tag{15c}$$

for $\sigma_k = (\sigma_k)^{n+1/2}_j$, $k = 1, 2, 3$.

By replacing (11a) and (11b) by (12) and (14) respectively, we obtain an implicit system that the classic CE-SE method simplifies by means of the following approximation [1],

$$\tilde{s}_k(j, n+1/2) = \frac{\tilde{s}_k(j-1/2, n) + \tilde{s}_k(j+1/2, n)}{2}, \qquad k = 1, 2, 3, \tag{16}$$

being the CE-SE an explicit numerical scheme. The essence of the semi-implicit scheme [5] is to eliminate this approximation and to solve the resulting implicit system of the substitution of expressions (12) and (14) in integral form (11),

$$\begin{aligned}
&(\sigma_1)^{n+1/2}_j + \left[\frac{(\Delta t)\delta_j}{4}\right](\sigma_2)^{n+1/2}_j = L_1, \\
&(\sigma_2)^{n+1/2}_j + \left[\frac{2 f_r (\Delta t)}{4 D_j}\right]\left(\frac{\sigma_2}{\sigma_1}\right)^{n+1/2}_j |\sigma_2|^{n+1/2}_j + \left[\frac{(\Delta t)\delta_j}{4}\right]\left(\frac{\sigma_2^2}{\sigma_1}\right)^{n+1/2}_j = L_2, \\
&(\sigma_3)^{n+1/2}_j + \left\{\left[\frac{\gamma \delta_j \Delta t}{4}\right]\left(\frac{\sigma_2}{\sigma_1}\right)^{n+1/2}_j + \left[\frac{h(\gamma-1)(\Delta t)}{R D_j}\right](\sigma_1^{-1})^{n+1/2}_j\right\}(\sigma_3)^{n+1/2}_j \\
&\quad - \left[\frac{(\gamma-1)(\Delta t)\delta_j}{8}\right]\left(\frac{\sigma_2^3}{\sigma_1^2}\right)^{n+1/2}_j - \left[\frac{h(\gamma-1)(\Delta t)}{2 R D_j}\right]\left(\frac{\sigma_2^2}{\sigma_1^2}\right)^{n+1/2}_j = L_3 + \frac{h(\Delta t)}{D_j}(T_p)_j
\end{aligned} \tag{17}$$

where L_k, $k = 1, 2, 3$, are defined by known coefficients of the previous time step,

$$\begin{aligned}
L_k = &\frac{1}{2}\left[(\sigma_k)^n_{j+1/2} + (\sigma_k)^n_{j-1/2}\right] - \frac{(\Delta x)}{8}\left[(\alpha_k)^n_{j+1/2} - (\alpha_k)^n_{j-1/2}\right] \\
&- \frac{1}{(\Delta x)}\left[(g_k)^n_{j+1/2} - (g_k)^n_{j-1/2}\right] - \frac{(\Delta t)}{8}\left[(\tilde{s}_k)^n_{j+1/2} + (\tilde{s}_k)^n_{j-1/2}\right],
\end{aligned} \tag{18}$$

where $g_k(\cdot, t^n; \cdot, n)$ is defined by (13), (the notation $(\cdot)$ represents in each term the corresponding spatial component). From the first equation of system (17) we have,

$$(\sigma_1)^{n+1/2}_j = L_1 - \left[\frac{(\Delta t)\delta_j}{4}\right](\sigma_2)^{n+1/2}_j, \tag{19}$$

replacing this value in the second equation and arranging the resulting terms, it follows that

$$\left[\frac{f_r(\Delta t)}{2 D_j}\right](\sigma_2)^{n+1/2}_j \left|(\sigma_2)^{n+1/2}_j\right| + \left[L_1 + \frac{(\Delta t)\delta_j}{4} L_2\right](\sigma_2)^{n+1/2}_j = L_1 L_2, \tag{20}$$

whose resolution depends on the sign of the coefficient $(\sigma_2)_j^{n+1/2}$.

Disregarding friction, then the second order term disappears in (20) and this equation is easily solved. If friction is taken into account, then for obtaining real solutions of the equation with module (20), we require the CFL condition in each time step verifying Corollary 4.1. Separating (20) in two quadratic equations,

if $(\sigma_2)_j^{n+1/2} \geq 0$, then

$$\left[\frac{f_r(\Delta t)}{2D_j}\right](\sigma_2^2)_j^{n+1/2} + \left[L_1 + \frac{(\Delta t)\delta_j}{4}L_2\right](\sigma_2)_j^{n+1/2} - L_1L_2 = 0; \tag{21}$$

if $(\sigma_2)_j^{n+1/2} \leq 0$, then

$$\left[-\frac{f_r(\Delta t)}{2D_j}\right](\sigma_2^2)_j^{n+1/2} + \left[L_1 + \frac{(\Delta t)\delta_j}{4}L_2\right](\sigma_2)_j^{n+1/2} - L_1L_2 = 0. \tag{22}$$

Solving we obtain up to four possible solutions of equation (20). So, in case of having more than one value of $(\sigma_2)_j^{n+1/2}$, we have to choose one of them of an appropriate form. By (10) we know that $(\sigma_2)_j^{n+1/2} = \tilde{w}_2(x_j, t^{n+1/2}; j, n+1/2)$, then we approximate $\tilde{w}_2(x_j, t^{n+1/2}; j, n+1/2)$ by the following average,

$$\begin{aligned} m &= \frac{\tilde{w}_2(x_{j-1/2}, t^{n+1/2}; j-1/2, n) + \tilde{w}_2(x_{j+1/2}, t^{n+1/2}; j+1/2, n)}{2} \\ &= \frac{\left[(\sigma_2)_{j-1/2}^n + (\beta_2)_{j-1/2}^n(\Delta t/2)\right] + \left[(\sigma_2)_{j+1/2}^n + (\beta_2)_{j+1/2}^n(\Delta t/2)\right]}{2}, \end{aligned} \tag{23}$$

so that we select the value of $(\sigma_2)_j^{n+1/2}$, whose difference in module with respect to m is the smallest of all the obtained differences. We replace this value in (19) obtaining $(\sigma_1)_j^{n+1/2}$. With both coefficients we calculate $(\sigma_3)_j^{n+1/2}$ from the third equation of system (17).

In order to obtain the coefficients $(\alpha_k)_j^{n+1/2}$, $k=1,2,3$, we define 3 points in CE$(j, n+1/2)$, P_+, P, and P_-, corresponding to the coordinates $(x_{j+1/2}, t^{n+1/2})$, $(x_j, t^{n+1/2})$, and $(x_{j-1/2}, t^{n+1/2})$, respectively, as we show in Figure 2. Since $P_\pm$ do not belong to SE$(j \pm 1/2, n)$ the value of $\tilde{\omega}_k(P_\pm)$ is calculated in the point that is below P_+ and P_- in each corresponding SE. In case that a discontinuity of the solution occurs between P_+ and P but not between P and P_-, one would expect that $|(\alpha_{k+})_j^{n+1/2}| \gg |(\alpha_{k-})_j^{n+1/2}|$, where

$$(\alpha_{k\pm})_j^{n+1/2} = \pm\frac{\tilde{\omega}_k(P_\pm) - (\sigma_k)_j^{n+1/2}}{(\Delta x/2)} = \pm\frac{\left[(\sigma_k)_{j\pm1/2}^n + (\beta_k)_{j\pm1/2}^n((\Delta t)/2)\right] - (\sigma_k)_j^{n+1/2}}{(\Delta x/2)}, \tag{24}$$

are the lateral differences. As P and P_- are on the same side of the discontinuity, $(\alpha_k)_j^{n+1/2}$ should be closer to $(\alpha_{k-})_j^{n+1/2}$ than $(\alpha_{k+})_j^{n+1/2}$. This suggests that $(\alpha_k)_j^{n+1/2}$ should be a weighted average between $(\alpha_{k+})_j^{n+1/2}$ and $(\alpha_{k-})_j^{n+1/2}$, which gives more weight to the term with the smallest module,

$$\alpha_k = \begin{cases} \dfrac{|\alpha_{k+}|^c\,\alpha_{k-} + |\alpha_{k-}|^c\,\alpha_{k+}}{|\alpha_{k+}|^c + |\alpha_{k-}|^c}, & |\alpha_{k+}|^c + |\alpha_{k-}|^c \neq 0, \\ 0, & |\alpha_{k+}|^c + |\alpha_{k-}|^c = 0, \end{cases} \qquad k = 1,2,3, \tag{25}$$

where c is a positive real constant. In the boundary of the domain we calculate $(\alpha_k)_0^{n+1/2}$ using forward differences, $(\alpha_{k+})_0^{n+1/2}$, and $(\alpha_k)_M^{n+1/2}$ by means of backward differences, $(\alpha_{k-})_0^{n+1/2}$,

both defined in (24). Finally the coefficients $(\beta_k)_j^{n+1/2}$, $k = 1, 2, 3$, are obtained by replacing $\frac{\partial \tilde{f}_k}{\partial x}(x, t; j, n+1/2)$ and (15) in (10),

$$(\beta_1)_j^{n+1/2} = -\alpha_2 - \delta_j \sigma_2, \tag{26a}$$

$$(\beta_2)_j^{n+1/2} = -(\gamma - 1)\alpha_3 - \frac{\sigma_2}{\sigma_1}\left[\frac{(3-\gamma)}{2}\left(2\alpha_2 - \frac{\alpha_1\sigma_2}{\sigma_1}\right)\right] - \frac{\sigma_2}{\sigma_1}\left(\frac{2(f_r)}{D_j}|\sigma_2| + \delta_j\sigma_2\right), \tag{26b}$$

$$\begin{aligned}(\beta_3)_j^{n+1/2} = {} & -\gamma\frac{\sigma_3}{\sigma_1}\left(\frac{\sigma_2\alpha_3}{\sigma_3} + \alpha_2 - \frac{\sigma_2\alpha_1}{\sigma_1} + \delta_j\sigma_2\right) - \frac{(\gamma-1)}{2}\frac{\sigma_2^2}{\sigma_1^2}\left(2\frac{\sigma_2\alpha_1}{\sigma_1} - 3\alpha_2 - \delta_j\sigma_2\right) \\ & - \frac{4h}{D_j}\left[\frac{(\gamma-1)}{2}\left(2\frac{\sigma_3}{\sigma_1} - \frac{\sigma_2^2}{\sigma_1^2}\right) - (T_p)_j\right],\end{aligned} \tag{26c}$$

where $\sigma_k = (\sigma_k)_j^{n+1/2}$ and $\alpha_k = (\alpha_k)_j^{n+1/2}$, $k = 1, 2, 3$.

Once we know the coefficients $(\sigma_k)_j^{n+1/2}$, $(\alpha_k)_j^{n+1/2}$, and $(\beta_k)_j^{n+1/2}$, $k = 1, 2, 3$, the solution (9) is defined in each $\mathrm{SE}(j, n+1/2)$ and we have completed half time step of integration.

In the resolution of tapered problems appearing nonsmooth changes of the cross section area of the duct, we apply the developed semi-implicit numerical scheme with a technique that smooths the profile of the duct. So that the lack of mass conservation of the numerical solution is diminished. This smooth technique consists in changing the diameter of nodes where the derivative does not exist. In these points the diameter is substituted by the arithmetic average of the adjacent points. This technique is characterized by the alternated structure from the mesh points of the space-time region.

4. EXISTENCE OF REAL SOLUTION

In this section, we show that the existence of real solutions of (20) depends on the discretization of the space-time domain.

LEMMA 4.1. *Let $Q(\alpha)$ be the polynomial,*

$$Q(\alpha) = q_1\alpha + q_2\alpha^2 + q_3\alpha^3, \tag{27}$$

where $q_l \in \mathbb{R}$, $l = \{1, 2, 3\}$. Then, there exists $\alpha \in (0, 1]$, such that

$$Q(\alpha) \leq 1. \tag{28}$$

PROOF. Taking

$$0 < \alpha \leq \min\left\{1, \frac{1}{|q_1| + |q_2| + |q_3|}\right\}, \tag{29}$$

expression (28) is verified.

THEOREM 4.1. *The equation (20) has a real solution $(\sigma_2)_j^{n+1/2}$ if $(\Delta t)_n$ is adequately small $\forall n$.*

PROOF. The existence of real solution for (20) is tested verifying the following inequality,

$$4\left(\pm\frac{f_r(\Delta t)}{2D_j}L_1L_2\right) \leq \left(L_1 + \frac{(\Delta t)}{2}\delta_j L_2\right)^2, \tag{30}$$

where L_1 and L_2 are defined by (18).

Using algebraic operations on the previous inequality we have the following equivalent expression,

$$\frac{(\Delta t)L_1L_2\theta_j}{(L_1)^2 + (((\Delta t)/4)\delta_j L_2)^2} \leq 1, \tag{31}$$

where

$$\theta_j := \left(\pm\frac{2fr}{D_j} - \frac{\delta_j}{2}\right).$$

Our next goal is to obtain an upper bound of the left-hand side of inequality (31) with the following steps.

(i) Both terms of the denominator are positive. We eliminate $(((\Delta t)/4)\delta_j L_2)^2$ and obtain the following upper bound

$$\frac{(\Delta t)L_1L_2\theta_j}{(L_1)^2 + (((\Delta t)/4)\delta_j L_2)^2} \leq \frac{(\Delta t)L_2\theta_j}{L_1}. \tag{32}$$

(ii) We express L_1 and L_2 by polynomials of Δx and Δt:

$$\begin{aligned} L_1 &= a_1 + a_2(\Delta x) + a_3\frac{(\Delta t)}{(\Delta x)} + a_4\frac{(\Delta t)^2}{(\Delta x)} + a_5(\Delta t), \\ L_2 &= b_1 + b_2(\Delta x) + b_3\frac{(\Delta t)}{(\Delta x)} + b_4\frac{(\Delta t)^2}{(\Delta x)} + b_5(\Delta t), \end{aligned} \tag{33}$$

where a_s and b_s, $s = \{1,2,3,4,5\}$, are the coefficients obtained from (18). We replace (33) in the left-hand side of inequality (32),

$$\begin{aligned} \frac{(\Delta t)L_2\theta_j}{L_1} &= \theta_j\left[\frac{b_1(\Delta t)(\Delta x) + b_2(\Delta t)(\Delta x)^2 + b_3(\Delta t)^2 + b_4(\Delta t)^3 + b_5(\Delta t)^2(\Delta x)}{a_1(\Delta x) + a_2(\Delta x)^2 + a_3(\Delta t) + a_4(\Delta t)^2 + a_5(\Delta t)(\Delta x)}\right] \\ &\leq \theta_j\left[\frac{b_1(\Delta x)^2\alpha + b_2(\Delta x)^3\alpha + b_3(\Delta x)^2\alpha^2 + b_4(\Delta x)^3\alpha^3 + b_5(\Delta x)^3\alpha^2}{a_1(\Delta x) + a_2(\Delta x)^2 + a_3(\Delta x)\alpha + a_4(\Delta x)^2\alpha^2 + a_5(\Delta x)\alpha}\right], \end{aligned} \tag{34}$$

where $\alpha = \Delta t/\Delta x$.

Arranging the right-hand side of inequality (34) and writing the resulting expression in terms of α in the form,

$$\frac{A\alpha + B\alpha^2 + C\alpha^3}{D + E\alpha + F\alpha^2} \tag{35}$$

where A, B, C, D, E, and F are real coefficients.

If we prove,

$$\frac{A\alpha + B\alpha^2 + C\alpha^3}{D + E\alpha + F\alpha^2} \leq 1, \tag{36}$$

then, we have that

$$\frac{(\Delta t)L_1L_2\theta_j}{(L_1)^2 + (((\Delta t)/4)\delta_j L_2)^2} \leq \frac{(\Delta t)L_2\theta_j}{L_1} \leq \frac{A\alpha + B\alpha^2 + C\alpha^3}{D + E\alpha + F\alpha^2} \leq 1, \tag{37}$$

and the existence of real solution for equation (20) is proved. The expression (36) is equivalent to

$$A\alpha + B\alpha^2 + C\alpha^3 \leq D + E\alpha + F\alpha^2 \tag{38}$$

or

$$\frac{1}{D}\left[(A-E)\alpha + (B-F)\alpha^2 + C\alpha^3\right] \leq 1. \tag{39}$$

The inequality (39) is satisfied by Lemma 4.1.

COROLLARY 4.1. *Assuming the CFL condition (7) in each time step, we have that*

$$\alpha = \frac{\Delta t}{\Delta x} = \frac{\tau}{\max_{x_j}(|u| + |a|)}, \qquad \forall x_j, \quad j = 0, \ldots, M, \quad 0 < \tau \leq 1. \tag{40}$$

Therefore, we obtain real solutions for the equation (20) whenever the parameter τ is taken so that α verifies (29).

5. NUMERICAL RESULTS

Some numerical tests were carried out in order to evaluate the accuracy of the new method in terms of conservation law. A model that can reproduce an impulse test rig, [6], has been used to obtain the numerical results. Two different nonreflecting boundary conditions were adopted in order to simulate the phenomena that take place upstream and downstream of the modelled zone. In the upstream boundary condition, a pressure impulse has been imposed by means of the characteristics. The downstream boundary condition used was an anechoic edge. The goal was to avoid interference on the fluid dynamic behavior due to the edges of the ducts.

The geometrical characteristics of the tapered ducts calculated are shown in Table 1 where the length and diameter described correspond with the tapered ducts drawn in Figure 3. The angles chosen are similar to those that may appear in the ducts of a two-stroke engine.

Table 1. Geometrical configuration.

Configuration	Angle (°)	L1 - L3 (m)	D1 (m)	L2 (m)	D2 (m)
1C	3.0	0.5	0.033	0.16	0.016
2C	6.3	0.5	0.051	0.16	0.016
1D	3.0	0.5	0.016	0.16	0.033
2D	6.3	0.5	0.016	0.16	0.051

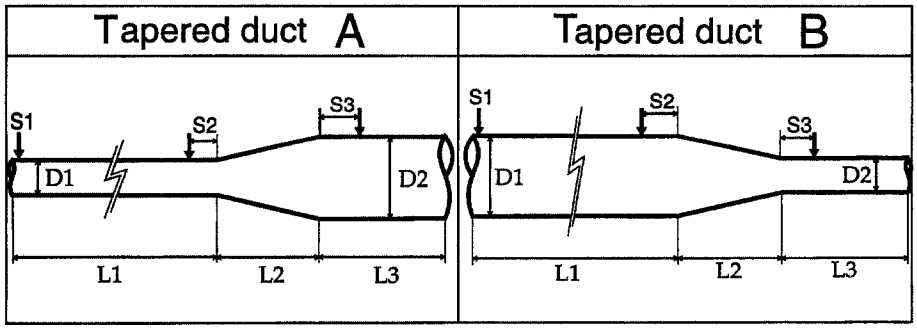

Figure 3. Profile of the conical ducts.

Due to the pressure impulse generated on one edge of the modelled system, a mass flow pulse is also generated. If the initial and final thermodynamic conditions inside the duct are the same, the integral of the mass flow pulse will be the same in every duct position. This integral has been calculated at every node along the duct.

The numerical results are shown in Figures 4 and 5. These figures represent the error between the air mass flow, (AMF), calculated at every node, and the mean air mass flow, (MAMF), of the original CE-SE method over the proposed scheme. Only the nodes around the tapered ducts have been plotted. The error on mass conservation has been observed with either the original or the new method when the section of the duct is constant. As can be observed in the results provided by the original method, when the duct diameter decreases, the air mass flow calculated increases. The original CE-SE method shows this behavior as much in convergent ducts as in divergent ones and is more important when the conical angle of the duct is increased.

On the other hand, the figures presented show how the new method reduces this behavior considerably providing more conservative results. These results demonstrate the importance of how the source term of the hyperbolic system is approximated.

It is also interesting to remark that the original CE-SE method has extremely important problems at the nodes placed at the beginning and end of the tapered duct due to the not existing derivative of the area at these points [8]. These problems can be minimized by means of a simple smooth technique applied to the duct profile. This technique has also been implemented in the variation of the CE-SE method proposed in this paper.

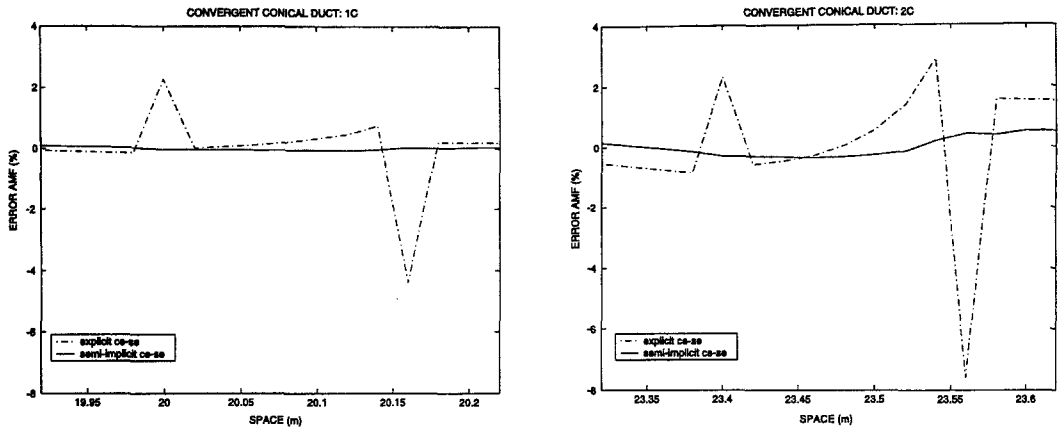

Figure 4. Convergent conical ducts: error AMF front MAMF for $\Delta x = 0.02\,\mathrm{m}$ and $\mathrm{CFL} = 0.9$.

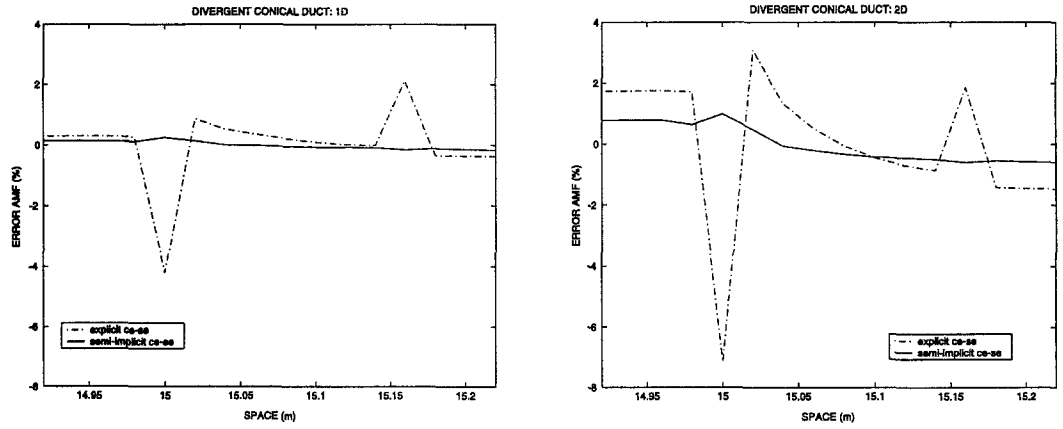

Figure 5. Divergent conical ducts: error AMF front MAMF for $\Delta x = 0.02\,\mathrm{m}$ and $\mathrm{CFL} = 0.9$.

As a conclusion, the new version proposed considerably improves the mass conservation under pulsating flow in tapered ducts and presents enough accuracy to be implemented in a wave action model.

REFERENCES

1. G. Briz and P. Giannattasio, Applicazione dello schema numerico conservation element-solution element al calcolo del flusso intazionario nei condotti dei motori a C.I., In *Proc. 48th ATI National Cong.*, pp. 233–247, Taomina, Italy, (1993).
2. S.C. Chang and W.M. To, A new numerical framework for solving conservation laws—The method of space-time conservation element and solution element, NASA TM 104495, (August 1991).
3. R.J. Pearson and D. E. Winterbone, The simulation of gas dynamics in engine manifolds using non-linear symmetric difference schemes, *Proc. Instn. Mech. Engrs. Part C: J. Mechanical Engineering Science* **211**, 601–616, (1997).
4. E.F. Toro, *Riemann Solvers and Numerical Methods for Fluid Dynamics*, Springer-Verlag, Berlin, (1997).
5. J.V. Romero, M.D. Roselló, S. Jerez and L. Jódar, *Solución Numérica de Sistemas de Leyes de Conservación para Conductos con Sección Variable, III Cong. Met. Num. Ing. y C. Apl., ITESM-CIMNE*, (Edited by S. Gallegos, I. Herrera, S. Botello, F. Zárate and G. Ayala), Monterrey, CA, January 22–24, 2004.
6. F. Payri, J.M. Desantes and A. Broatch, Modified impulse method for the measurement of the frecuency response of acoustic filters to weakly nonlinear transient excitations, *J. Acoust. Soc. Am.* **107** (2), (February 2000).
7. J.E. Marsden and A.J. Tromba, *Cálculo Vectorial*, Addison-Wesley, Iberoamericana, (1991).
8. F.J. Arnau, Aportaciones al cálculo numérico para el modelado del flujo comprensible unidimensional en conductos de M.C.I.A, Ph.D. Thesis, Departamento de Motores, Univ. Politécnica de Valencia, Spain, (2003).